

Preparation of silica-based proton conductors for intermediate temperature fuel cells

Dongho Seo, Sangsun Park, and Yong-Gun Shul[†]

Department of Chemical and Biomolecular Engineering, Yonsei University,
134 Shinchon-dong, Seodaemun-gu, Seoul 120-749, Korea
(Received 8 May 2008 • accepted 31 December 2008)

Abstract—The ternary system $\text{SiO}_2\text{-P}_2\text{O}_5\text{-ZrO}_2$ electrolyte and phosphotungstic acid (PWA) doped $\text{SiO}_2\text{-P}_2\text{O}_5\text{-ZrO}_2$ electrolyte were prepared for intermediate temperature fuel cell by using sol-gel technique. These silica-based proton conductors were confirmed to be non-crystalline structure without phase separation and good thermal stability by XRD and TG/DTA analysis. The doped PWA was found to be stabilized within the silica matrix and to enhance the proton conductivity. The proton conductivities of $\text{SiO}_2\text{-P}_2\text{O}_5\text{-ZrO}_2$ and $\text{SiO}_2\text{-P}_2\text{O}_5\text{-ZrO}_2\text{-PWA}$ electrolytes showed 3.3×10^{-5} and $1.8 \times 10^{-3} \text{ S/cm}$ at 90°C , respectively, and the cell performance of $\text{SiO}_2\text{-P}_2\text{O}_5\text{-ZrO}_2\text{-PWA}$ electrolyte was obtained as $0.02\text{-}0.25 \text{ mA/cm}^2$ at 300°C under humid condition.

Key words: Proton Conductor, Intermediate Temperature Fuel Cell, Sol-gel, PWA

INTRODUCTION

Solid proton conducting materials are attracting much attention due to having potential practical applications in clean energy fields such as fuel cells, batteries, sensors, and electrolysis, etc. [1,2]. The properties of solid-state electrolytes can be summarized in terms of proton conductivity and stability of various operation conditions. Recently, considerable research efforts have been devoted to develop the fuel cell at temperatures between 200 and 500°C , which is a promising operating temperature range for both material science and energy conversion processes [3]. Although a wide variety of proton conducting materials have already been proposed for the electrolytes, the development of chemically and thermally stable proton conductors still remains a prime open subject in fuel cell development [4-6]. A number of advanced features should be expected for operating PEMFC at temperature range of $150\text{-}300^\circ\text{C}$ due to promoting the electrode kinetics and enhanced durability of Pt catalyst by CO poisoning [7].

The sol-gel derived silica based glasses membranes have been reported for proton conducting materials as thermally stable electrolyte for fuel cells [8]. The hydroxyl groups such as Si-OH, P-OH and Zr-OH on the pore surfaces of inorganic oxides are bonded with water molecules, and the proton conduction is associated with proton hopping between hydroxyl bonds and water molecules [9-11]. Uma et al. have reported that proton conductivity of $\text{SiO}_2\text{-P}_2\text{O}_5\text{-ZrO}_2$ glasses was shown around $10^{-4}\text{-}10^{-3} \text{ S/cm}$ at temperature range of $30\text{-}90^\circ\text{C}$ [12]. The hydrogen in P-OH groups is more strongly hydrogen-bonded with water molecules than in Si-OH groups so that a high temperature is necessary to remove the water from P-OH, but phosphate lacks chemical and thermal durability. For this reason, introduction of cations such as Zr^{4+} into phosphosilicate glass improves chemical and mechanical stability [13].

The ion conductivity is proportional to the concentration of the mobile protons within the electrolyte. One of the approaches is used

to modify the membrane with an appropriate acidic solid, melt or solution of low volatility to increase proton conductivity [14]. In particular, hydrophilic additives such as phosphotungstic acid (PWA), zirconium phosphate (ZrP) and silicotungstic acid (SiWA) have shown significantly improved water retention property at higher temperature [15]. The basic structural unit of PWA is the Keggin anion ($\text{PW}_{12}\text{O}_{40}$)³⁻ which consist of the central PO_4 tetrahedron surrounded by four W_3O_{13} sets interconnected with hydrogen-bonded water molecules [16]. The PWA clusters stabilized within the silica network structure provide an acid-rich amorphous inorganic phase, so that the proton conduction can be facilitated through the polyacid-sites by Grotthus mechanism [17,18]. The presence of the PWA is expected to enhance the retention of the hydrated water and thus improve the proton conductivity even in a dry atmosphere. Nogami et al. reported that proton conductivity of about 10^{-2} S/cm was obtained by using $\text{P}_2\text{O}_5\text{-SiO}_2\text{-PWA}$ electrolytes at 90°C [19].

In this present study, we have successfully synthesized $\text{SiO}_2\text{-P}_2\text{O}_5\text{-ZrO}_2$ and PWA doped $\text{SiO}_2\text{-P}_2\text{O}_5\text{-ZrO}_2$ electrolytes by using sol-gel technique and investigated the thermal, chemical and electrochemical properties of these proton conductors for the application of intermediate temperature fuel cell. The silica-based proton conductors obtained by sintered process were a porous and crack-free transparent monolithic in features. The in-situ incorporated PWA was used to reinforce the proton mobility in silica network. The H_2/O_2 fuel cell performance using $\text{SiO}_2\text{-ZrO}_2\text{-P}_2\text{O}_5$ and $\text{SiO}_2\text{-ZrO}_2\text{-P}_2\text{O}_5\text{-PWA}$ electrolytes up to 300°C is discussed diligently.

EXPERIMENTAL

A schematic preparation method of silica-based electrolytes via the sol-gel process is shown in Fig. 1. A dilute solution of $\text{Si}(\text{OC}_2\text{H}_5)_4$ with $\text{C}_2\text{H}_5\text{OH}$ was pre-hydrolyzed with a solution of H_2O (0.1 N-HCl aq) in the molar ratio of 1 : 1 per mol of tetraethyl orthosilicate and stirred for 1 hour. A solution of $\text{Zr}(\text{OC}_4\text{H}_9)_4$ mixed with $\text{C}_2\text{H}_5\text{OH}$ in molar ratio of 1 : 5 was added, followed by stirring for 30 min. A solution of $\text{PO}(\text{OCH}_3)_3$ dissolved in $\text{C}_2\text{H}_5\text{OH}$ with five times moles was added drop by drop under stirred condition in the

[†]To whom correspondence should be addressed.
E-mail: shulyg@yonsei.ac.kr

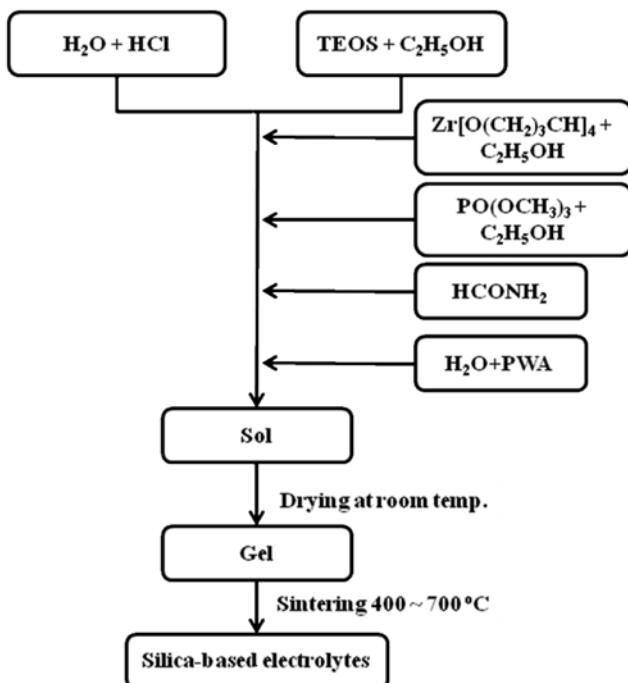


Fig. 1. Flow chart of synthesis for silica-based proton conductors by sol-gel method.

above solution. After 30 min stirring, 1 ml HCONH_2 was added per 5 g alkoxide solution for 30 min with continuous stirring. For the preparation of $\text{SiO}_2\text{-P}_2\text{O}_5\text{-ZrO}_2$ electrolyte, the mixture of precursor solutions was vigorously stirred for 1 hour to get a homogeneous solution at room temperature and the solution was poured into petri dish to form gel at room temperature for 2 months. The gel was sintered at 700°C for 5 hours to get completely condensed alkoxide. The $\text{H}_3\text{PW}_{12}\text{O}_{40}$ solution was prepared by deionized water with appropriate amount for the required stoichiometric for alkoxide hydrolysis and added to the above solution before the sol-gel formation on the petri dish. The PWA-doped silica-based electrolyte was obtained by using the same above-mentioned procedure except the gel was sintered at 400°C .

The average pore size, total pore volume and the specific surface area of synthesized electrolytes were determined by nitrogen adsorption technique using N_2 at 77 K (ASAP-2010, Micromeritics). X-ray diffraction patterns were recorded for the electrolytes powder by a Rigaku Denki D/max-IIIC instrument using Cu-K_α radiation in steps size of 0.02° and recorded from 5° to 60° . Thermogravimetric and differential thermal analysis (TG/DTA) data were obtained with a Shimadzu TA-50 series instrument with a heating rate of $20\text{ }^\circ\text{C}/\text{min}$ from room temperature to $800\text{ }^\circ\text{C}$ under N_2 atmosphere. The Fourier transform infra red spectroscopy (FTIR) data for the PWA, PWA doped and undoped $\text{SiO}_2\text{-P}_2\text{O}_5\text{-ZrO}_2$ were collected with an ATR system (Smiths, Travel IR). The catalyst slurry was prepared by mixing Pt/C (60% Pt, E-TEK) powder with isopropanol and silica sol. The catalyst slurry was pasted on gold-coated Ni-sponge and dried at $80\text{ }^\circ\text{C}$ for 1 day to remove the solvents from the catalyst layer. The active surface area of the electrode was 0.38 cm^2 . The membrane electrode assembly (MEA) was mounted in a single cell, and assembled by four screws carefully. A schematic representation of MEA and single cell for fuel cell performance is presented in Fig. 2. The proton conductivity was measured with an impedance analyzer (Autolab, PGSTAT-30). Impedance spectra were recorded in a frequency range from 0.1 Hz to 10 kHz with voltage amplitude of 10 mV in fully humidified hydrogen and oxygen. The performance of the cells was measured by multimeter (Keithley, 2000) connected to a power supply (Agilent, 6060B) at $\sim 300\text{ }^\circ\text{C}$ and cell temperature was controlled by heating stick. Flow rate of hydrogen and oxygen was 50 ml/min with fully humidified conditions and Pt loading was about 0.1 mg/cm^2 for anode and cathode respectively.

RESULTS AND DISCUSSION

The dried gels at room temperature were clear and crack-free monolithic features. During the sintering process, the gels were shrunk due to dehydration-condensation of the hydroxyl groups, and the transformation occurs in the gel to highly transparent and yellow colored silica-based electrolytes (thickness about $0.5\text{-}1\text{ mm}$), as shown in Fig. 3. The high transparency indicates that all the components were blended homogeneously at molecular level and PWA clusters were incorporated in silica gel matrix. N_2 adsorption-desorption iso-

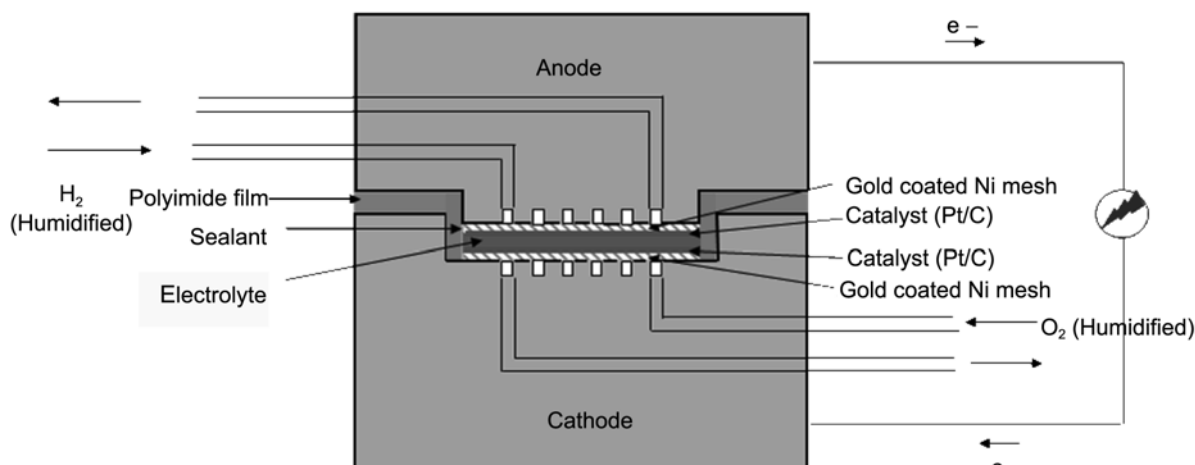


Fig. 2. Schematic of the single cell for H_2/O_2 fuel cell.

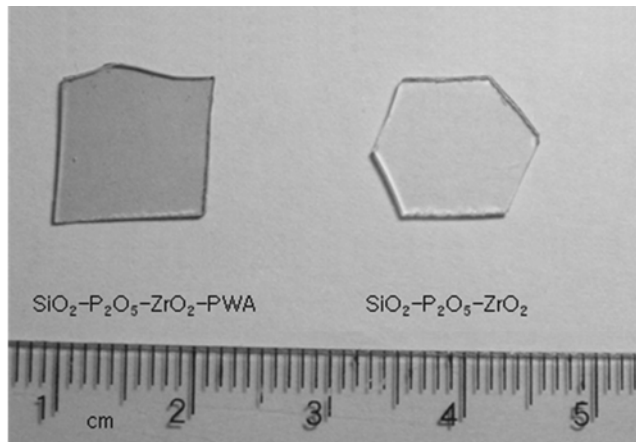


Fig. 3. Photograph of $\text{SiO}_2\text{-P}_2\text{O}_5\text{-ZrO}_2$ and $\text{SiO}_2\text{-P}_2\text{O}_5\text{-ZrO}_2\text{-PWA}$ samples.

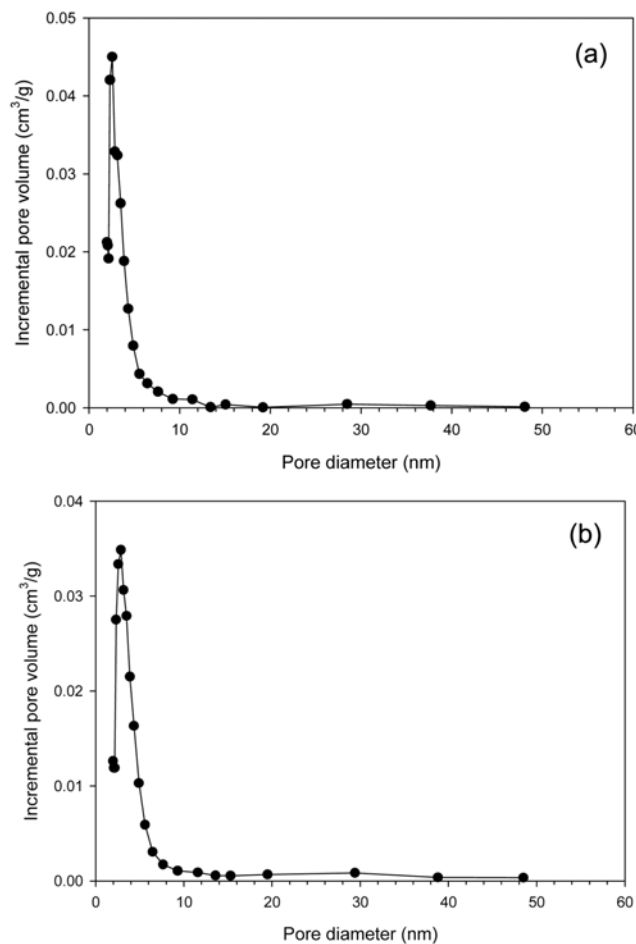


Fig. 4. Pore size distribution for the (a) $\text{SiO}_2\text{-P}_2\text{O}_5\text{-ZrO}_2$ and (b) $\text{SiO}_2\text{-P}_2\text{O}_5\text{-ZrO}_2\text{-PWA}$ samples.

therms and pore size distribution of two different type samples are shown in Fig. 4. The composition and surface properties of these electrolytes are summarized in Table 1. The specific surface area and pore volume of PWA doped $\text{SiO}_2\text{-P}_2\text{O}_5\text{-ZrO}_2$ are smaller than in $\text{SiO}_2\text{-P}_2\text{O}_5\text{-ZrO}_2$ electrolytes, on the other hand, the average pore size is large. This suggests that the PWA clusters were entrapped in the nanopore of silica electrolytes homogeneously.

The XRD patterns of pure PWA, $\text{SiO}_2\text{-P}_2\text{O}_5\text{-ZrO}_2$ and $\text{SiO}_2\text{-P}_2\text{O}_5\text{-ZrO}_2\text{-PWA}$ electrolytes are shown in Fig. 5. It shows only one broad peak at 2θ values around 20–35° which is an indication of the typical amorphous silicate characteristics of the electrolytes. No X-ray diffraction peak for PWA appeared in the spectrum of $\text{SiO}_2\text{-P}_2\text{O}_5\text{-ZrO}_2\text{-PWA}$ electrolyte, only a little shift of broad peak towards the right side. This behavior suggests that the dispersed PWA interacts well with silanols from silica, which is the cause for the formation of amorphous structure.

TG/DTA curves for the $\text{SiO}_2\text{-P}_2\text{O}_5\text{-ZrO}_2$ and $\text{SiO}_2\text{-P}_2\text{O}_5\text{-ZrO}_2\text{-PWA}$ samples are shown in Fig. 6. A drastic weight loss (about 17%) was observed between 20 °C and 100 °C with an endothermic peak of around 70 °C in both of the samples. This weight loss can be attributed to the evaporation of residual alcohols and water molecules. The consequent weight losses (about 12–15%) up to ~350 °C are due to the removal of more structural water from PWA, organic solvents and water generated during the sol-gel reactions. The weight loss rates are lower above 350 °C, but continuous up to 800 °C. An exothermic peak at 40 °C in the DTA curve at is due to the decomposition of the silane molecule chains that are bonded to the silica network. A broad exothermic peak was observed at about 650 °C without noticeable weight loss in Fig. 4(b), it is assigned to the partial decomposition of the heteropoly acid sites [20].

The FTIR transmittance spectra for the pure PWA, $\text{SiO}_2\text{-P}_2\text{O}_5$ -

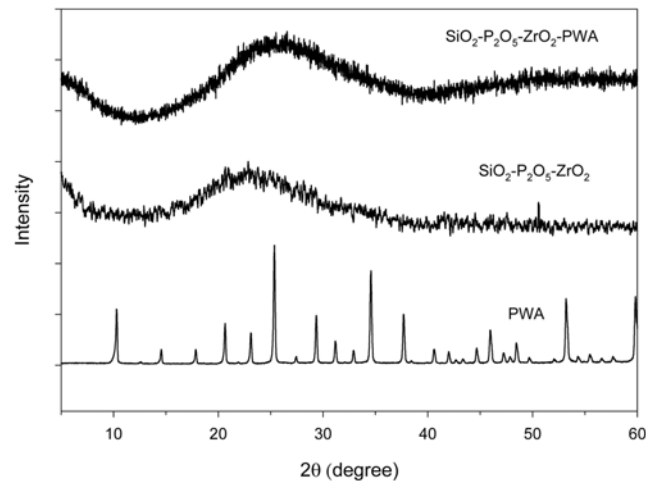


Fig. 5. XRD patterns of the pure PWA, $\text{SiO}_2\text{-P}_2\text{O}_5\text{-ZrO}_2$ and $\text{SiO}_2\text{-P}_2\text{O}_5\text{-ZrO}_2\text{-PWA}$ samples.

Table 1. Composition, synthesis condition and properties of $\text{SiO}_2\text{-P}_2\text{O}_5\text{-ZrO}_2$ and $\text{SiO}_2\text{-P}_2\text{O}_5\text{-ZrO}_2\text{-PWA}$ samples

Sample	Composition (mol%)	Sintering temp. (°C)	Specific surface area (m^2/g)	Pore volume (cm^3/g)	Pore radius (nm)
$\text{SiO}_2\text{-P}_2\text{O}_5\text{-ZrO}_2$	80 : 10 : 10	700	716	0.32	2.3
$\text{SiO}_2\text{-P}_2\text{O}_5\text{-ZrO}_2\text{-PWA}$	84 : 10 : 5 : 1	400	518	0.26	2.5

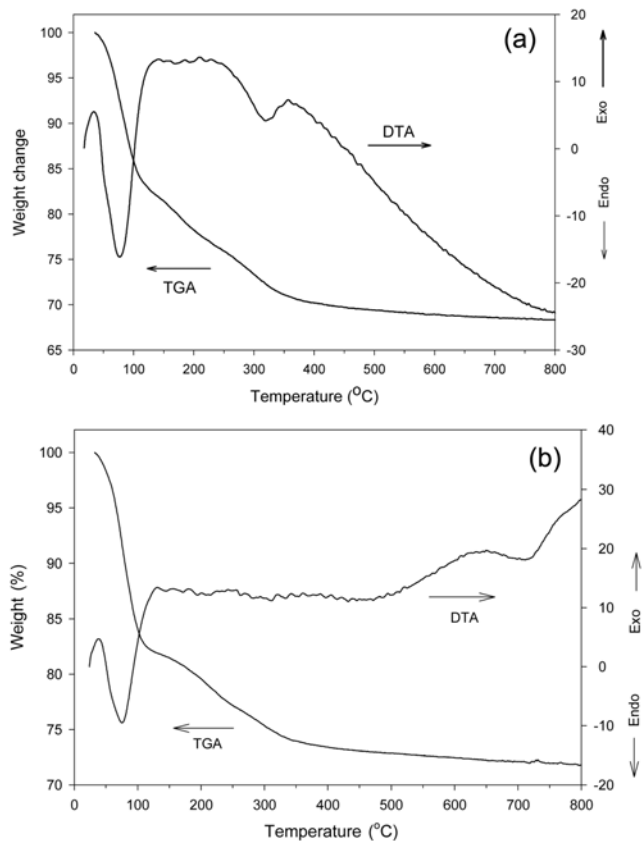


Fig. 6. TGA/DTA curve for the (a) $\text{SiO}_2\text{-P}_2\text{O}_5\text{-ZrO}_2$ and (b) $\text{SiO}_2\text{-P}_2\text{O}_5\text{-ZrO}_2\text{-PWA}$ samples.

ZrO_2 and $\text{SiO}_2\text{-P}_2\text{O}_5\text{-ZrO}_2\text{-PWA}$ electrolytes are presented in Fig. 7. A broad band in the range $3,200\text{-}3,500\text{ cm}^{-1}$ is attributed to the vibration of water (H-O-H) and a band at $3,750\text{ cm}^{-1}$ represents the $\text{Si}-\text{O}-\text{H}$ silanols with hydrogen. The main characteristic of the silica matrix can be identified by FTIR analysis. The $\text{Si}-\text{O}-\text{Si}$ stretching vibrations are observed at around $1,050\text{ cm}^{-1}$ and 800 cm^{-1} . A shoulder at around 950 cm^{-1} is assigned to the $\text{Si}-\text{O}-\text{Zr}$ or $\text{Si}-\text{O}-\text{P}$ vibration. There is a shoulder at around $1,200\text{ cm}^{-1}$ that has been attributed to

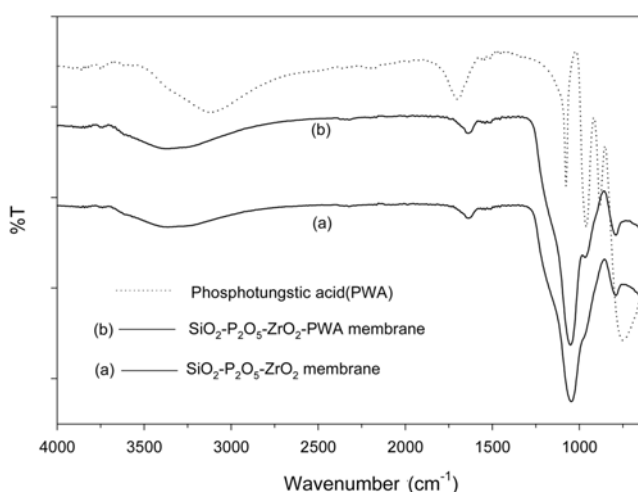


Fig. 7. FT-IR spectra of the pure PWA, $\text{SiO}_2\text{-P}_2\text{O}_5\text{-ZrO}_2$ and $\text{SiO}_2\text{-P}_2\text{O}_5\text{-ZrO}_2\text{-PWA}$ samples.

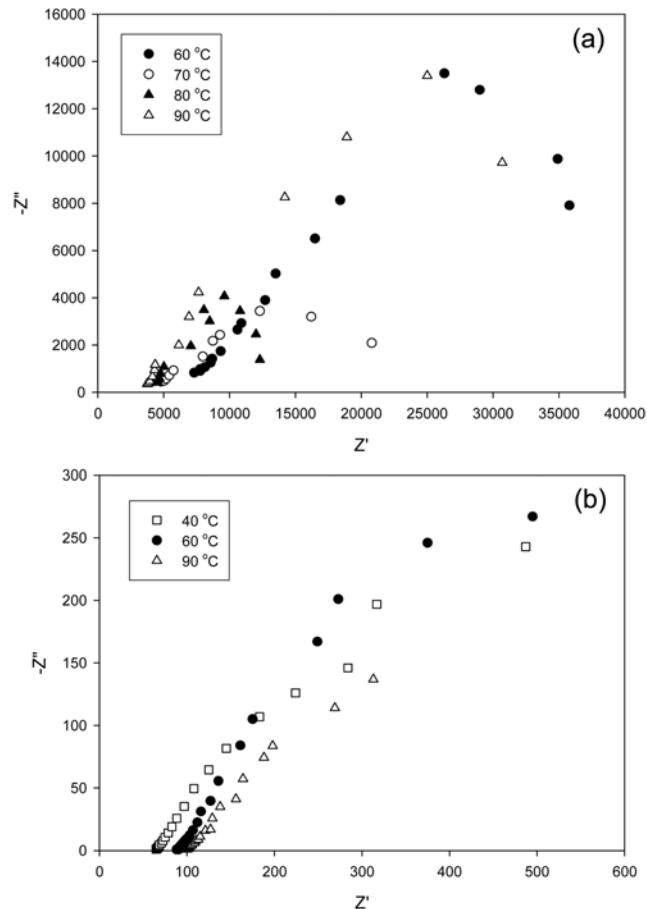


Fig. 8. Impedance curves of (a) $\text{SiO}_2\text{-P}_2\text{O}_5\text{-ZrO}_2$ and (b) $\text{SiO}_2\text{-P}_2\text{O}_5\text{-ZrO}_2\text{-PWA}$ samples at different temperatures.

P=O stretching. The bands at $1,650\text{ cm}^{-1}$ in the spectrum are assigned to the deformation modes of OH and adsorbed water molecular in the pores surface. The band position of pure PWA at 770 cm^{-1} , 900 cm^{-1} , 950 cm^{-1} and $1,060\text{ cm}^{-1}$ is assignment of the corner-sharing $\text{W}-\text{O}_c\text{-W}$, edge-sharing $\text{W}-\text{O}_b\text{-W}$, terminal $\text{W}-\text{O}_d$ and $\text{P}-\text{O}_a$ respectively, which are representing fingerprints of the Keggin unit structure (Fig. 6 PWA). There is a stronger intensive peak at 950 cm^{-1} in spectrum for the $\text{SiO}_2\text{-P}_2\text{O}_5\text{-ZrO}_2\text{-PWA}$ electrolyte than $\text{SiO}_2\text{-P}_2\text{O}_5\text{-ZrO}_2$ electrolyte, which is due to the effect of PWA interacting with silica framework. The other peaks of Keggin anion are hidden by the peaks of silica structure.

Fig. 8 shows the impedance curves for these prepared electrolytes taken at different temperatures. The semicircle represents a typical equivalent circuit of a resistor and capacitor connected in parallel corresponding to the bulk electrochemical properties. The proton conductivity σ of the samples was calculated from the impedance data, using the relation of $\sigma=t/\text{RS}$. Where, t and S are the thickness and electrode area of the specimens, respectively. R is the resistance obtained from the extrapolated intersection of high-frequency semi-circle in the real axis (Z'). The proton conductivity as a function of temperature for these silica-based electrolytes is given in Fig. 9. A conductivity of around 10^{-5} S/cm and 10^{-3} S/cm was measured for the $\text{SiO}_2\text{-P}_2\text{O}_5\text{-ZrO}_2$ and the $\text{SiO}_2\text{-P}_2\text{O}_5\text{-ZrO}_2$ electrolytes at temperatures range of $40\text{-}90\text{ }^\circ\text{C}$, respectively. The introduc-

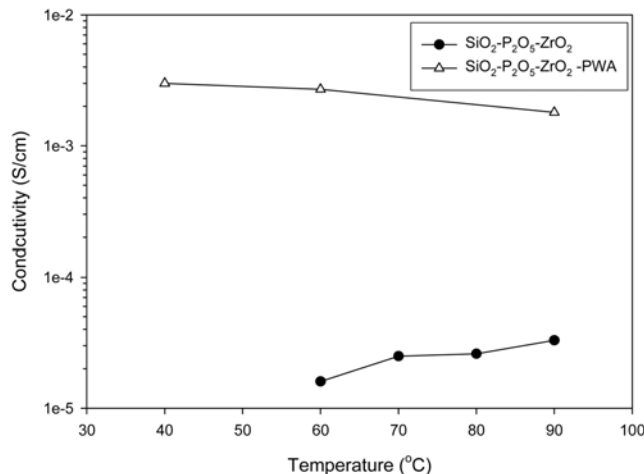


Fig. 9. Conductivity of $\text{SiO}_2\text{-P}_2\text{O}_5\text{-ZrO}_2$ and $\text{SiO}_2\text{-P}_2\text{O}_5\text{-ZrO}_2\text{-PWA}$ samples as a function of temperature.

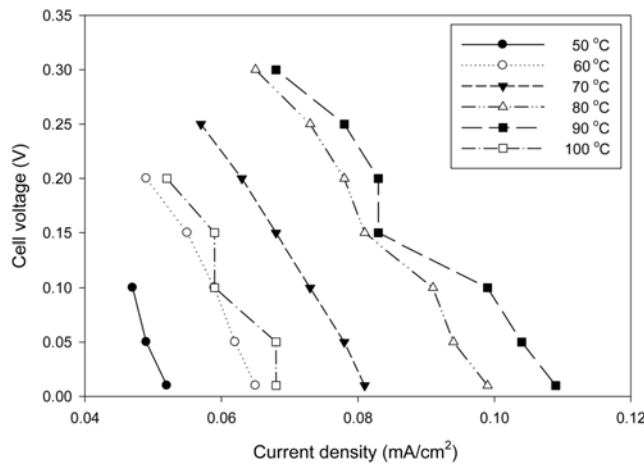


Fig. 10. Performance of unit cell using the $\text{SiO}_2\text{-P}_2\text{O}_5\text{-ZrO}_2$ sample at different temperatures.

tion of PWA into the silica framework remarkably improved the proton conductivity about two orders of magnitude as high as that of unmodified silica membrane.

Fig. 10 shows I-V curves of the $\text{SiO}_2\text{-P}_2\text{O}_5\text{-ZrO}_2$ electrolyte at different operational temperatures. The open circuit voltage of 0.1–0.3 V and current density of 0.07–0.15 mA/cm^2 were recorded using $\text{SiO}_2\text{-P}_2\text{O}_5\text{-ZrO}_2$ electrolyte at temperature between 50 and 100 °C. It seems that the OCV and performance of the H_2/O_2 fuel cell is low; this result may be due to the large interfacial charge transfer resistance. Fig. 11 shows I-V curves of the $\text{SiO}_2\text{-P}_2\text{O}_5\text{-ZrO}_2\text{-PWA}$ electrolytes at different operational temperatures. The open circuit voltage of 0.3–0.7 V and current density of 0.02–0.25 mA/cm^2 were recorded by using $\text{SiO}_2\text{-P}_2\text{O}_5\text{-ZrO}_2\text{-PWA}$ electrolyte at a temperature range of 40–300 °C. The OCV and current densities of the PWA doped silica electrolyte are greater than unmodified silica electrolyte.

CONCLUSIONS

We have successfully prepared $\text{SiO}_2\text{-P}_2\text{O}_5\text{-ZrO}_2$ and PWA doped

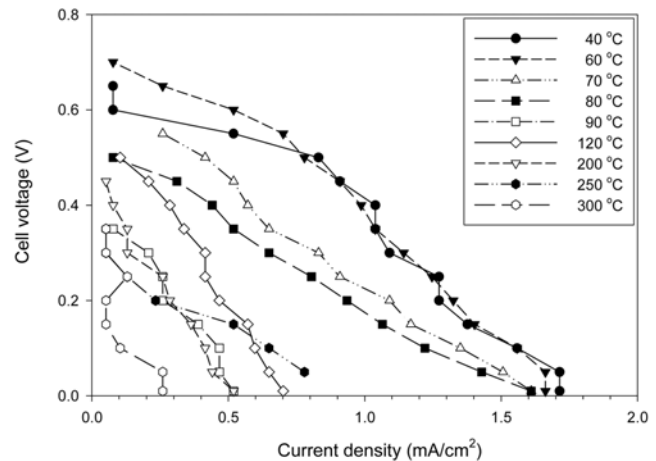


Fig. 11. Performance of unit cell using the $\text{SiO}_2\text{-P}_2\text{O}_5\text{-ZrO}_2\text{-PWA}$ sample at different temperatures.

$\text{SiO}_2\text{-P}_2\text{O}_5\text{-ZrO}_2$ electrolytes by sol-gel process. These synthesized proton conductors were found to be homogeneous nanoporous structure and thermally stable up to 800 °C. The proton conductivities of $3.3 \times 10^{-5} \text{ S/cm}$ and $1.8 \times 10^{-3} \text{ S/cm}$ were obtained from $\text{SiO}_2\text{-P}_2\text{O}_5\text{-ZrO}_2$ and $\text{SiO}_2\text{-P}_2\text{O}_5\text{-ZrO}_2\text{-PWA}$ electrolytes at 90 °C, respectively. The increase of conductivity should be attributed to the presence of PWA in the silica matrix. The cell performance of 0.07–0.15 mA/cm^2 at 90 °C and 0.02–0.25 mA/cm^2 at 300 °C was obtained from $\text{SiO}_2\text{-P}_2\text{O}_5\text{-ZrO}_2$ and $\text{SiO}_2\text{-P}_2\text{O}_5\text{-ZrO}_2\text{-PWA}$ electrolytes under humid conditions, respectively. The modification of silica-based proton conductor with PWA was found to improve the cell performance and have a potential for fuel cell application at operating temperature around 300 °C.

ACKNOWLEDGMENT

This work was supported by Brain Korea 21 project and the fostering project of the Specialized Graduate School of Hydrogen & Fuel Cell supported financially by the Ministry of Commerce, Industry and Energy (MOCIE).

REFERENCES

1. G. Alberti and M. Casciola, *Solid State Ionics*, **145**, 3 (2001).
2. B. Nakrupai, K. Pruksathom and P. Piemsomboon, *Korean J. Chem. Eng.*, **23**, 570 (2006).
3. T. Norby, *Solid State Ionics*, **125**, 1 (1999).
4. S. M. Haile, *Acta Materialia*, **51**, 5981 (2003).
5. J. Zhang, Z. Xie, J. Zhang and S. Holdcroft, *Journal of Power Sources*, **160**, 872 (2006).
6. D. H. Seo, H. R. Kim, P. Shakthivel and Y. G. Shul, *Journal of the Korea Electrochemical Society*, **11**, 22 (2008).
7. J. S. Wainright, M. H. Litt and R. F. Savinell, *Handbook of Fuel Cells*, **3**, 436 (2003).
8. Y. Abe, M. Hayashi, T. Iwamoto, H. Sumi and L. L. Hench, *Journal of Non-Crystalline Solid*, **351**, 2138 (2005).
9. Y. Daiko, T. Akai, T. Kasuga and M. Nogami, *Journal of the Ceramic Society of Japan*, **109**, 815 (2001).

10. M. Nogami, R. Nagao, W. Cong and Y. Abe, *Journal of Sol-Gel Science and Technology*, **13**, 933 (1998).
11. M. Aparicio and L. C. Klein, *Journal of Sol-Gel Science and Technology*, **28**, 199 (2003).
12. T. Uma and M. Nogami, *Materials Chemistry and Physics*, **98**, 382 (2006).
13. Y. Castro, M. Aparicio, R. Moreno and A. Duran, *Journal of Sol-Gel Science and Technology*, **35**, 41 (2005)
14. N. L. Garland and J. P. Kopasz, *Journal of Power Sources*, **172**, 94 (2007).
15. U. Mioc, M. Davidovic, N. Tjapkin, Ph. Colombar and A. Novak, *Solid State Ionics*, **46**, 103 (1991)
16. P. Staiti, S. Freni and S. Hocevar, *Journal of Power Sources*, **79**, 250 (1999).
17. M. Aparicio, Y. Castro and A. Duran, *Solid State Ionics*, **176**, 333 (2005).
18. I. Honma, Y. Takeda and J. M. Bae, *Solid State Ionics*, **120**, 255 (1999).
19. T. Uma and M. Nogami, *Journal of Membrane Science*, **280**, 744 (2006).
20. Y. Izumi, M. Ogawa and K. Urabe, *Appl. Catal. A: General*, **132**, 127 (1995).